

## Supporting information

### Quick in-situ generation quinone-enrich surface of N-doped carbon cloth electrode for electric double-layer capacitors

Xiaowei Lv,<sup>a</sup> Shan Ji,<sup>\*b</sup> Jun Lu,<sup>a</sup> Lei Zhang,<sup>a</sup> Xuyun Wang<sup>a</sup> and Hui Wang<sup>\*a</sup>

<sup>a</sup> State Key Laboratory Base for Eco-Chemical Engineering, College of Chemical Engineering, Qingdao University of Science and Technology, Qingdao 266042, China

<sup>b</sup> College of Biological, Chemical Science and Chemical Engineering, Jiaxing University, Jiaxing 314001, China

#### Physical characterizations

The images of scanning electron microscopy (SEM) were taken on JSM-6330F. The SL200B instrument was used to measure the surface wettability of different samples. X-ray photoelectron spectra (XPS) was acquired with a VG Escalab210 spectrometer fitted with Mg 300 W X-ray source. Energy dispersive spectroscopy (EDS) was employed for determining the elemental composition. The specific surface area was determined by Brunauere-Emmette-Teller (BET) method and the pore size distribution was calculated by the density functional theory (DFT) method using the model slit pore, NLDFT equilibrium model on a Quantachrome Autosorb-1 volumetric analyzer. The absorbance of visible light was measured with a UV-5800 (PC) ultraviolet-visible spectrophotometer.

## Electrochemical measurements

All electrochemical tests of the as-prepared samples were evaluated on the CHI 660E electrochemical workstation. The obtained sample (size: 1×1 cm<sup>2</sup>), platinum foil, Ag/AgCl (saturated KCl) were employed as the working electrode, the counter electrode, and the reference electrode respectively. H<sub>2</sub>SO<sub>4</sub> (1 M) was used as the electrolyte for all electrochemical tests. Electrochemical impedance spectrum was measured from 0.01 to 1,000,000 Hz.

Area specific capacitance (C<sub>a</sub>), volume specific capacitance (C<sub>v</sub>), energy density (E) and power density (P) were calculated by the following equations:

$$C_a = I \times t / (A \times \Delta V) \quad (1)$$

$$C_v = I \times t / (V \times \Delta V) \quad (2)$$

$$E = C_v \times (\Delta U)^2 / 2 \quad (3)$$

$$P = E / \Delta t \quad (4)$$

in which I, t, ΔV, V and A are discharge current (A), discharge time (s), potential window (ΔV), electrode volume (cm<sup>3</sup>) and electrode area (cm<sup>2</sup>).

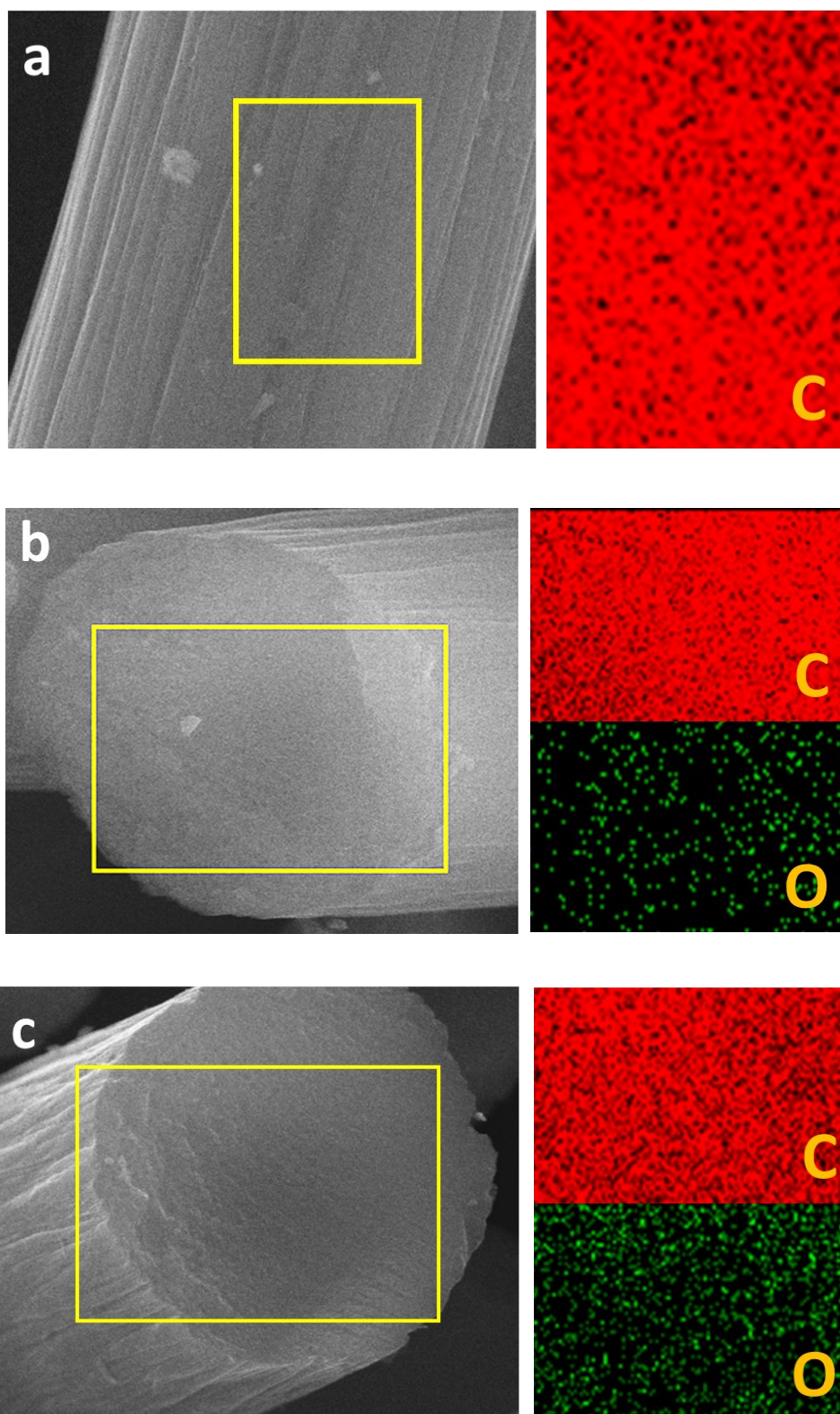


**Figure S1.** SEM image and the element mapping image of a selected region of (a) CC, (b) N-CC and (c) EO-N-CC.

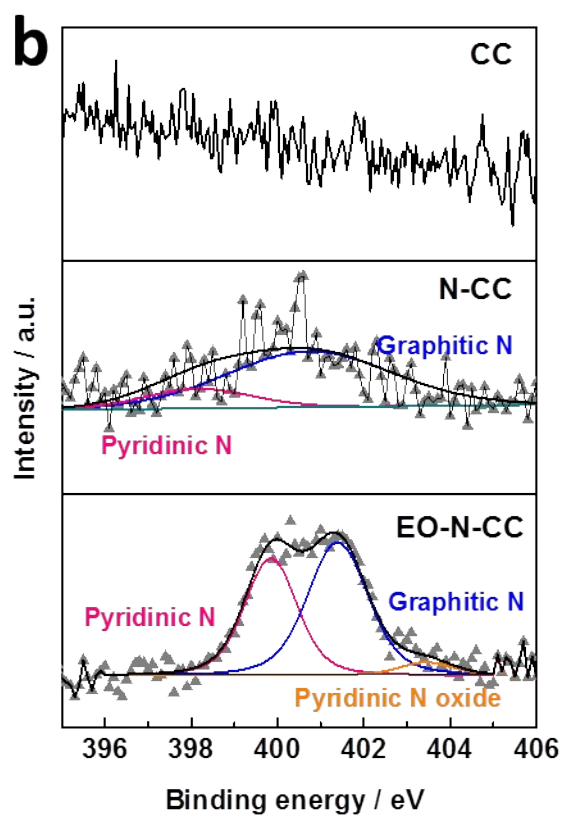
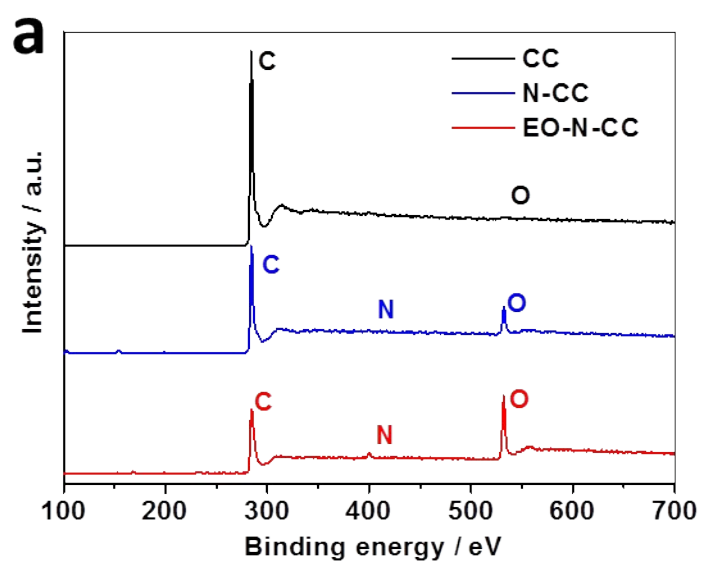


**Figure S2.** (a) XPS survey spectra and (b) N 1s XPS spectra of CC, N-CC, and EO-N-CC.

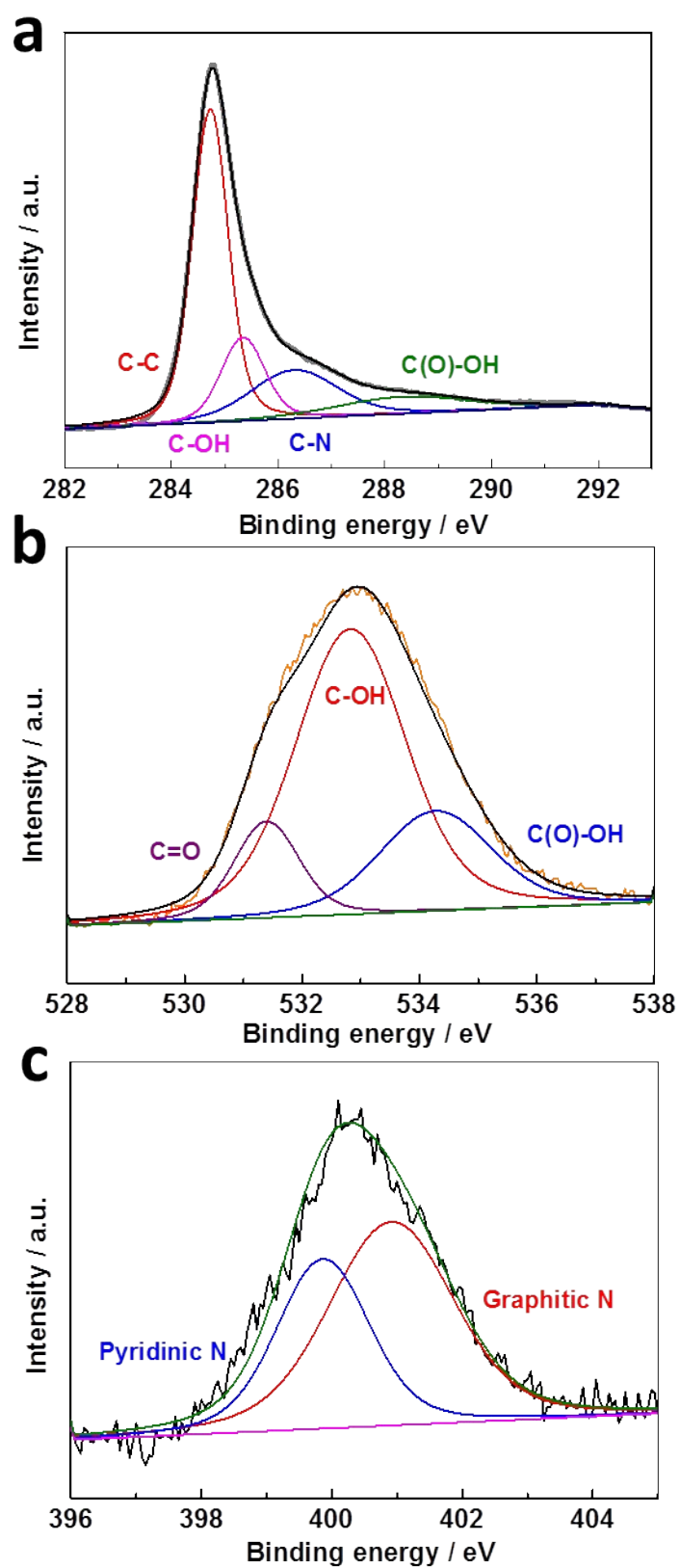


**Figure S3.** (a) C 1s, (b) O 1s, and (c) N 1s XPS spectra of CO-N-CC.

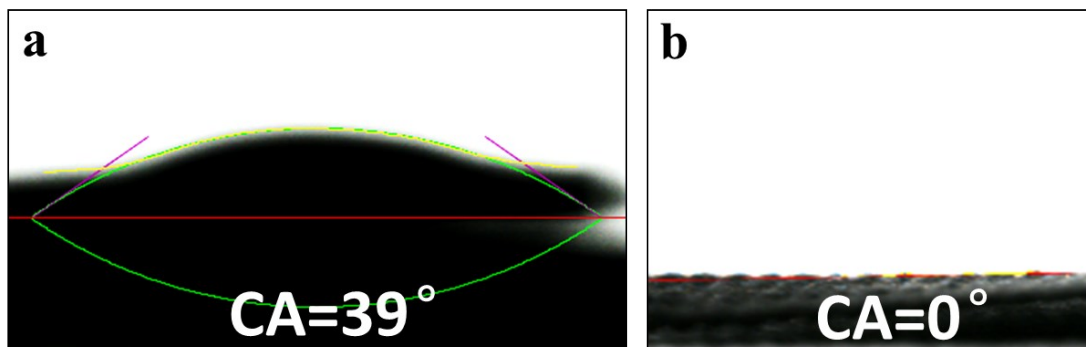


**Figure S4.** The contact angles of (a) CO-N-CC prepared by chemical oxidation and (b) EO-CC prepared by electrochemical oxidation.

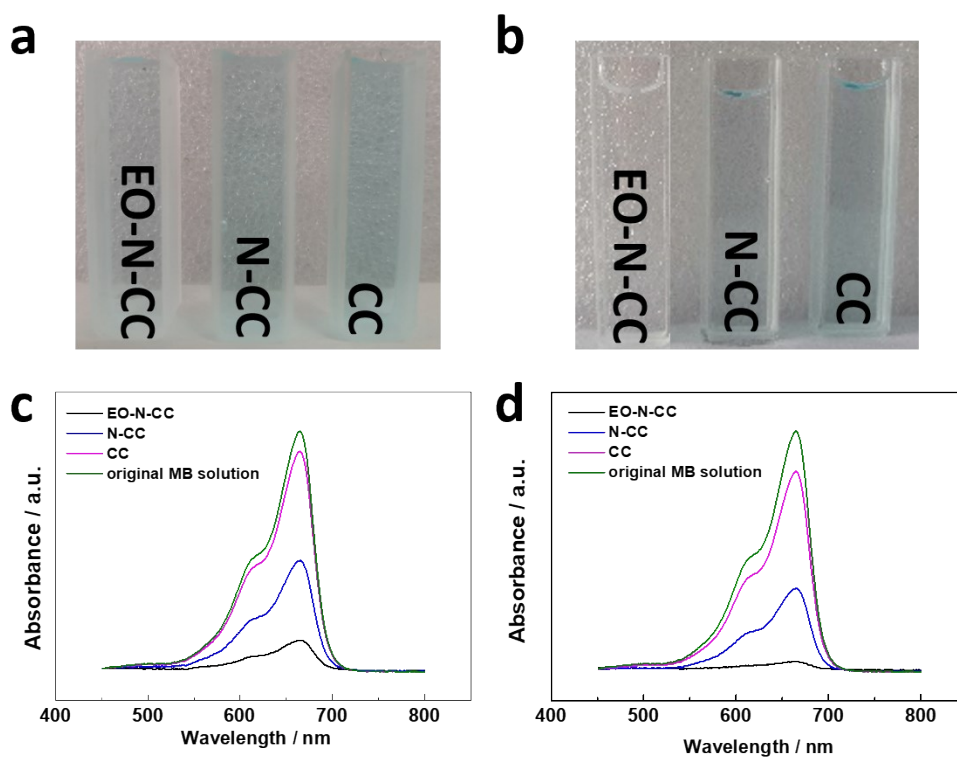


**Figure S5.** (a) the difference of the color of the remaining methylene blue solution after stirring without light for 6 h; (b) the difference of the color of the remaining methylene blue solution after stirring without light for 12 h. The ultraviolet absorption spectrum of the remaining solution after stirring for (c) 6h and (d) 12h.

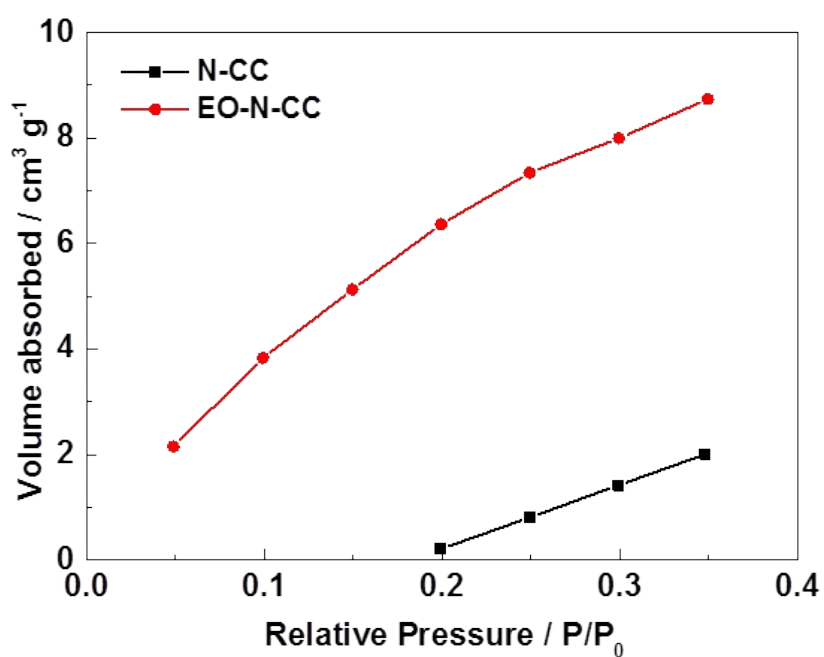


Figure S6. N<sub>2</sub> adsorption isotherm of EO-N-CC and N-CC below P/P<sub>0</sub> of 0.35.

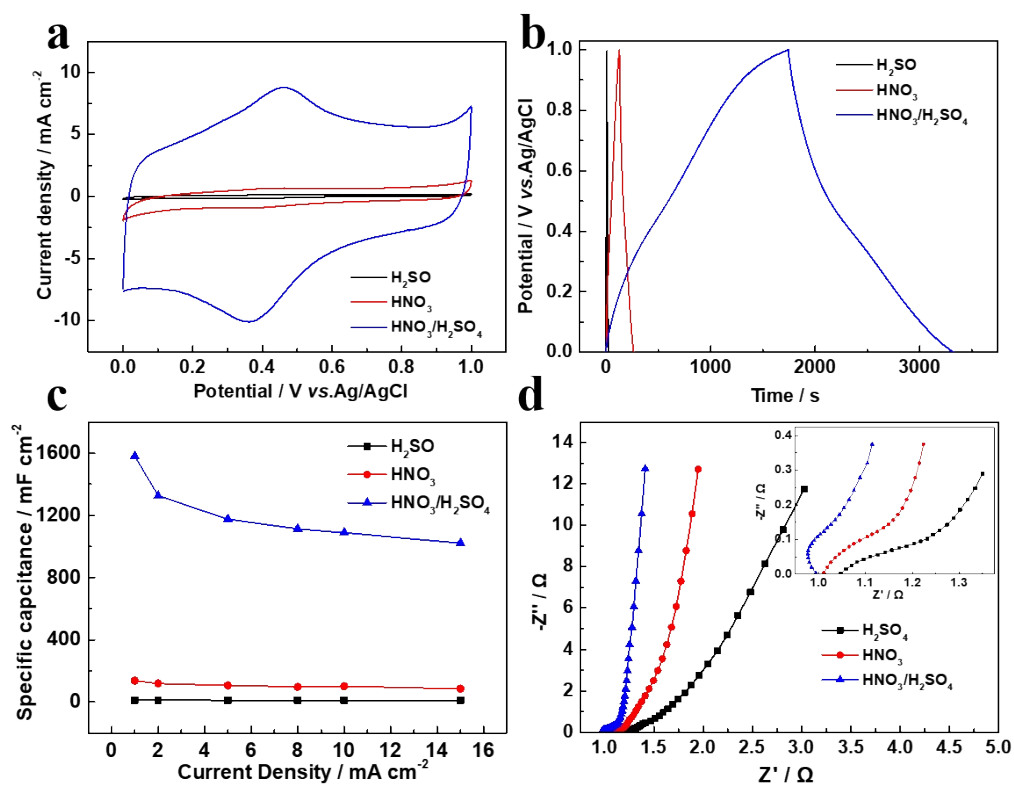
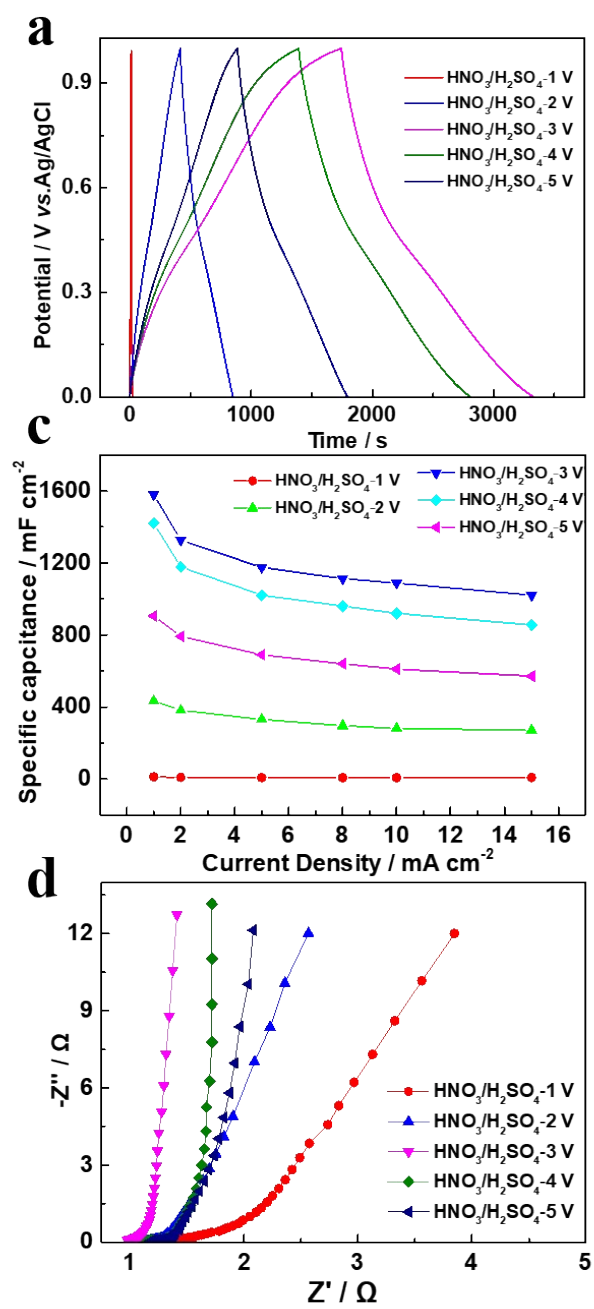


Figure S7. (a) Cyclic voltammetry at 5 mV s<sup>-1</sup>. (b) galvanostatic charge and discharge at 10 mA cm<sup>-2</sup>.

1 mA cm<sup>-2</sup>. (c) area-specific capacitance. (d) electrochemical impedance spectroscopy of the samples oxidized in different acid solutions.

The volume ratio of H<sub>2</sub>SO<sub>4</sub> and HNO<sub>3</sub> was 1:1 (20 mL). Since 1 mol of concentrated H<sub>2</sub>SO<sub>4</sub> can absorb up to 4 mol of H<sub>2</sub>O, 20 mL of 68% concentrated HNO<sub>3</sub> contains 0.5 mol of water, and needs 6.6 mL of concentrated H<sub>2</sub>SO<sub>4</sub> to absorb water. If only using 6.6 mL of concentrated H<sub>2</sub>SO<sub>4</sub>, but the water absorption rate is low, so the amount of concentrated sulfuric acid was increased to 20 mL and the results found that 1:1 is an appropriate ratio for our experiments.





**Figure S8.** (a) galvanostatic charge and discharge at 1 mA cm<sup>-2</sup>. (b) area-specific capacitance. (c) electrochemical impedance spectroscopy of the samples oxidized with various applied potentials.

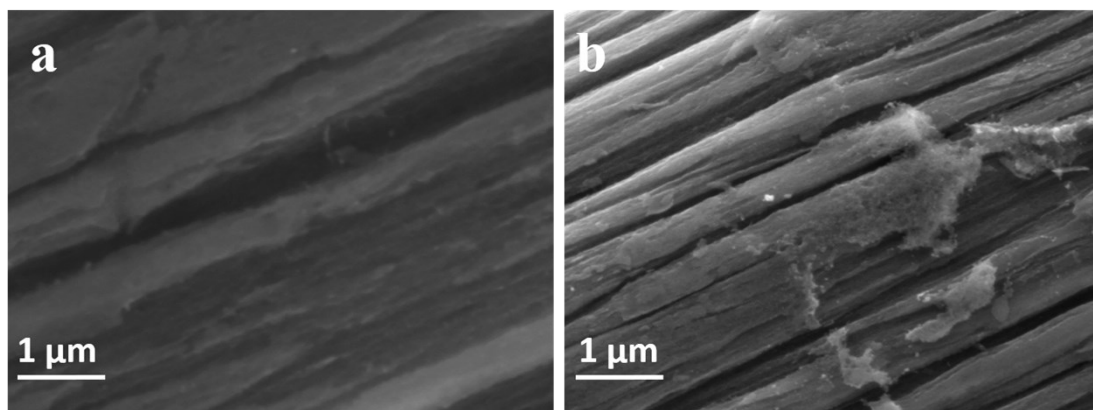


**Figure S9.** SEM images of the samples via electric oxidation at (a) 1 V and (b) 5 V.

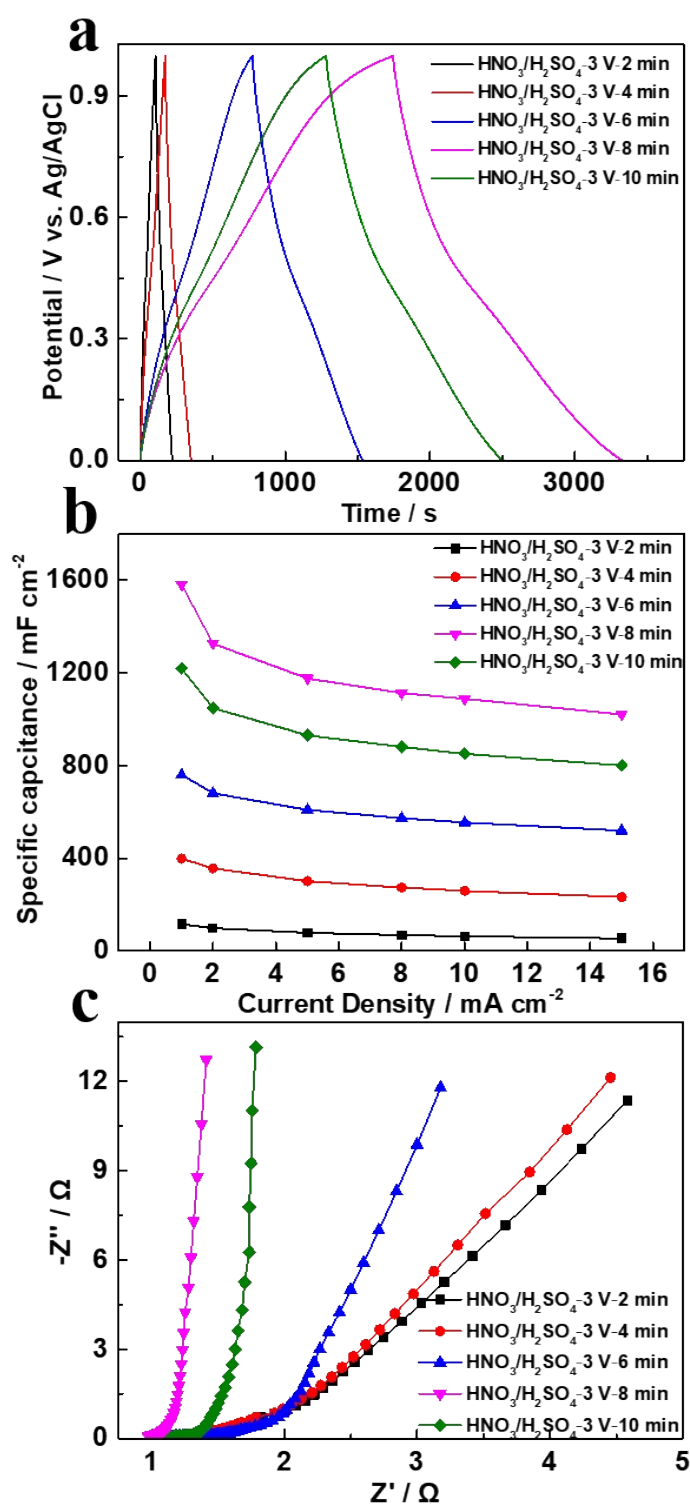


**Figure S10.** (a) Galvanostatic charge and discharge at 1 mA cm<sup>-2</sup>. (b) Area-specific capacitance. (c) Electrochemical impedance spectroscopy of the samples oxidized with different times at 3V.

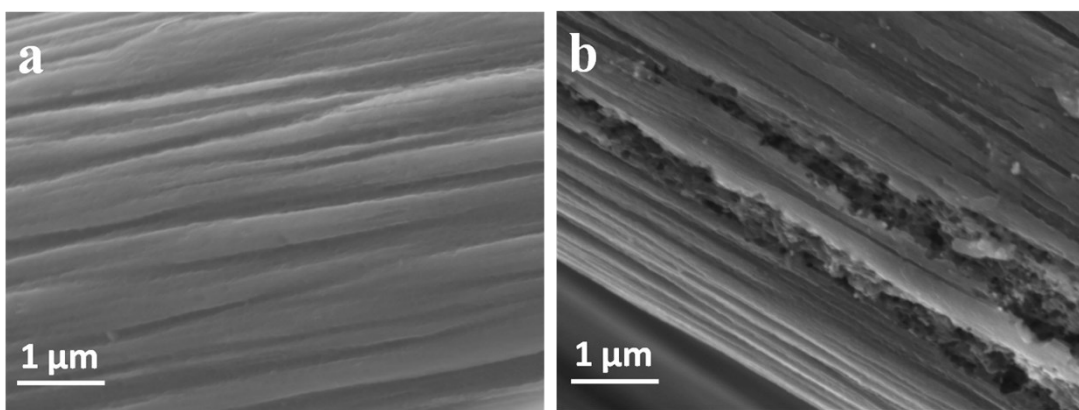


**Figure S11.** SEM images of the samples via electric oxidation at 3 V with the time of (a) 2 min and (b) 10 min.

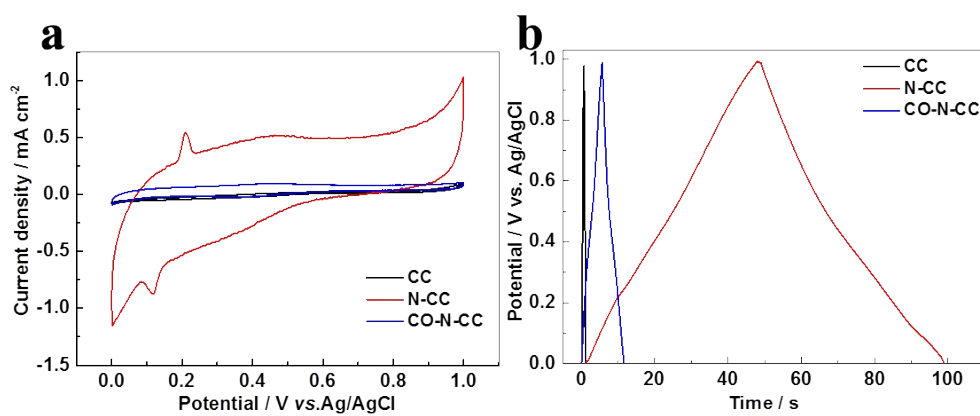


**Figure S12.** (a) The cyclic voltammetry curve of CC, N-CC, CO-N-CC at  $5 \text{ mV s}^{-1}$  and (b) galvanostatic charge and discharge of CC, N-CC, CO-N-CC at  $1 \text{ mA cm}^{-2}$ .

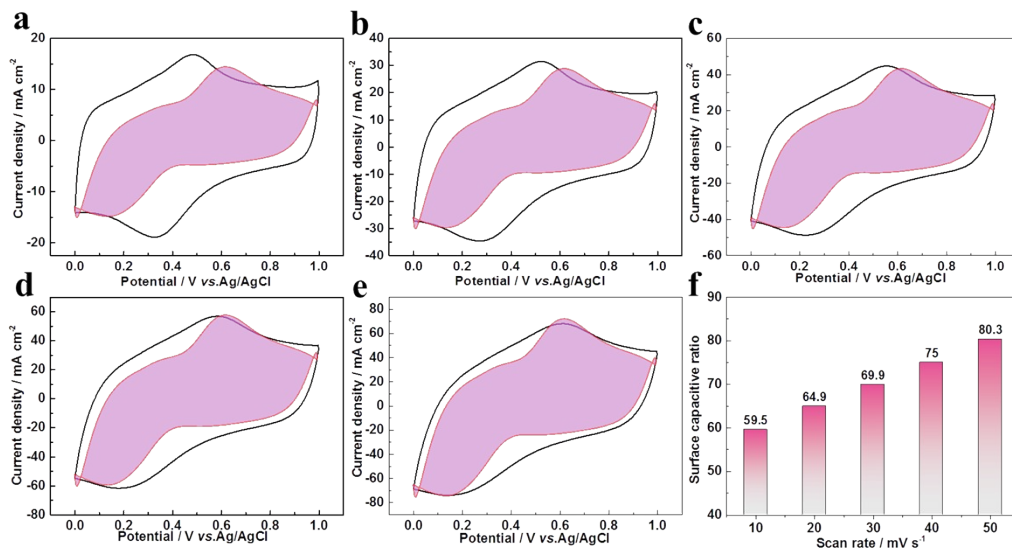


**Figure S13.** (a-e) Fitting graph of double-layer capacitance contribution of EO-N-CC at scan rates of 10, 20, 30, 40, and 50 mV s<sup>-1</sup>. (f) The proportion of surface capacitance contribution.

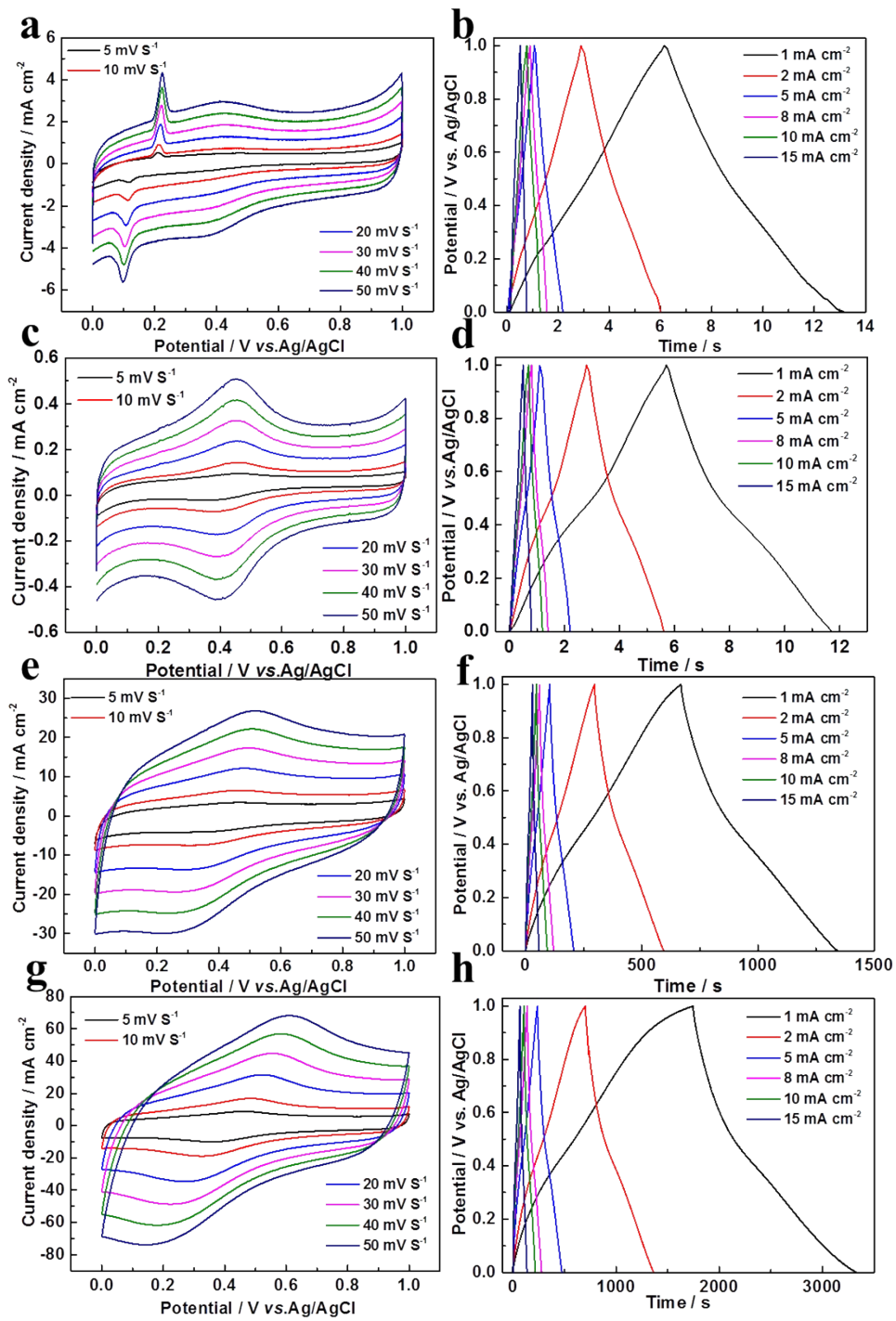
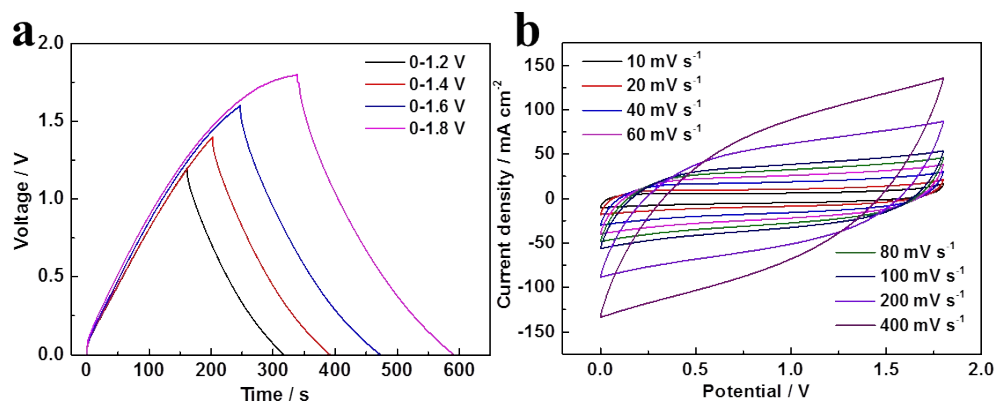


Figure S14. CVs and GCDs of (a,b) N-CC, (c,d) CO-N-CC, (e,f) EO-CC and (g,h) EO-N-CC.



**Figure S15.** (a) GCD curves at different voltage windows (at  $5 \text{ mA cm}^{-2}$ ). (b) CV curves of symmetric capacitor at different scan rates from  $10$  to  $400 \text{ mV s}^{-1}$ .



**Figure S16.** A photographic image of the device's power supply LED.

The method of preparing  $\text{H}_2\text{SO}_4$ -polyvinyl alcohol (PVA) gel electrolyte is as follows:  $6 \text{ g}$  of  $\text{H}_2\text{SO}_4$  was mixed with  $60 \text{ ml}$  of deionized water, and then add  $6 \text{ g}$  of PVA powder. The mixture was heated to  $95^\circ\text{C}$  under vigorous stirring until the solution becomes clear. The solution was then maintained at  $95^\circ\text{C}$  for  $1 \text{ h}$ .

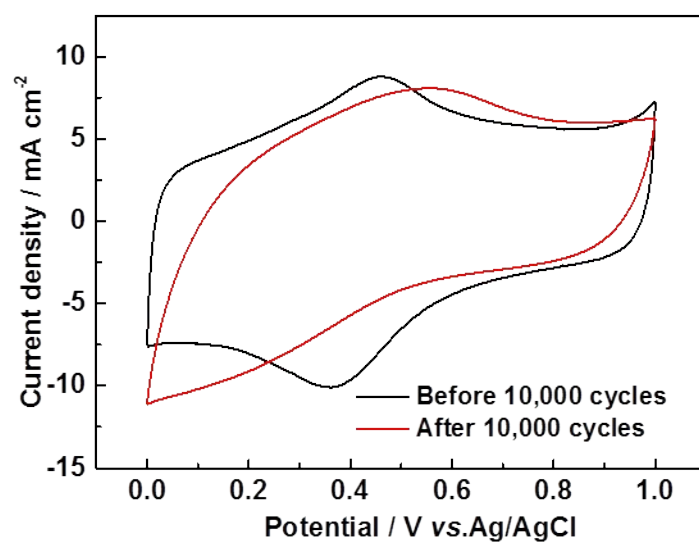


**Figure S17.** CVs at 5 mV s<sup>-1</sup> of EO-N-CC after 10,000 cycles.



**Table S1.** The content of OCFG in N-CC, CO-N-CC and EO-N-CC based on the fitted peak areas of O 1s XPS.

Sample \ OCFG	C=O	>COH	-COOH
N-CC	905.9	695.3	473.3
CO-N-CC	3221.7	6142.5	2115.5
EO-N-CC	5222.3	8734.1	4000.0

**Table S2.**  $R_S$  and  $R_{CT}$  of CC, N-CC, CO-N-CC, EO-CC, EO-N-CC.

	CC	N-CC	CO-N-CC	EO-CC	EO-N-CC
$R_{CT}(\Omega)$	17.523	5.498	32.84	4.856	2.46
$R_S(\Omega)$	1.523	1.087	1.1	1.044	1.013

**Table S3.** Benchmarking the capacitor performance of as-prepared carbon electrodes with the reported carbon electrodes in terms of specific capacitance, energy density, power density, and cycle life.

Electroactive material	Current density (mA cm <sup>-2</sup> )	Specific Capacitance (mF cm <sup>-2</sup> )	Energy density (mWhcm <sup>-3</sup> )	Power density (W cm <sup>-3</sup> )	Percentage	Cycle number	Reference
EO/CO-NC	1	1600	9.47	0.112	97%	10000	This work
EACC-10	6	756	1.5	1.71	no any decay	70000	[1]
APCFT	4	1200	4.7	2.29	no any decay	25000	[2]
CFC	2	500			no any decay	15 000	[3]
TCC	2	920	0.128				[4]
ACC	10	88			97%	20000	[5]
GOCC	0.5	327	0.556	1.016	no any decay	25000	[6]
A ECC	5	5310	4.27	1.32	93%	5000	[7]
aTC	5	1026			97	10000	[7]

#### Reference

1. W. Wang, W. Liu, Y. Zeng, Y. Han, M. Yu, X. Lu and Y. Tong, *Adv Mater*, 2015, 27, 3572-3578.
2. Y. Han, Y. Lu, S. Shen, Y. Zhong, S. Liu, X. Xia, Y. Tong and X. Lu, *Adv. Funct. Mater.*, 2019, 29, 1806329.
3. T. Zhang, C. H. Kim, Y. Cheng, Y. Ma, H. Zhang and J. Liu, *Nanoscale*, 2015, 7, 3285-3291.
4. H. Wang, J. Deng, C. Xu, Y. Chen, F. Xu, J. Wang and Y. Wang, *Energy Storage Materials*, 2017, 7, 216-221.
5. G. Wang, H. Wang, X. Lu, Y. Ling, M. Yu, T. Zhai, Y. Tong and Y. Li, *Adv Mater*, 2014, 26, 2676-2682.
6. S. Gao, L. Zhu, L. Liu, A. Gao, F. Liao and M. Shao, *Electrochim. Acta*, 2016, 191, 908-915.
7. Z. Miao, Y. Huang, J. Xin, X. Su, Y. Sang, H. Liu and J. J. Wang, *ACS Appl Mater Interfaces*, 2019, 11, 18044-18050.